Heliyon 6 (2020) e04784

Contents lists available at ScienceDirect

Heliyon

journal homepage: www.cell.com/heliyon

Research article

Characterization of polyamide-6/ propolis blended electrospun fibers

Bibi Marzieh Razavizadeh [a,*], Razieh Niazmand [b]

[a] Research Institute of Food Science and Technology, Department of Food Safety and Quality Control, Mashhad, Iran
[b] Research Institute of Food Science and Technology, Department of Food Chemistry, Mashhad, Iran

ARTICLE INFO

Keywords:
Materials science
Nanotechnology
Electrospinning
Polyamide-6
Blending
Propolis ethanolic extract

ABSTRACT

Polyamide-6 (PA-6) nanofibers and PA-6/propolis ethanolic extract (EEP) blended fibers were prepared having electrospun their solutions in formic acid as solvent. The effect of concentrations of PA-6 and also EEP in polymer solutions on the morphology and physicochemical characteristics of their electrospun fibers was investigated. The analysis of FESEM images showed the mean diameter of fibers increased from 487- 682 nm with increasing PA-6 concentration in the range of 25–40 % w/v. While, increasing EEP concentration (20–50% (w/w)) in PA-6/EEP system caused the increasing fiber mean diameters from 943- 1773 nm. Partially high aspect ratio nanofibers were observed only in the PA-6 systems. Antioxidant activity of the fibers enhanced with increasing EEP concentration in the fiber mats. FTIR spectrums and thermal properties of electrospun fibers exhibited the simple mixtures of PA-6 and EEP in blend fibers which did not contain very complex interactions.

1. Introduction

Nowadays, research about polymer-based composite materials has significantly grown. For this purpose, there are different techniques applied either by blending different polymers or by incorporating inorganic materials or natural effective compounds into polymers [1, 2, 3, 4, 5].

Regarding the simplicity and versatility of electrospinning method, this technique has been very much considered for producing nano and microfibers from a wide range of polymers in many applications such as textile engineering, pharmaceuticals, and filtration [6].

In electropinning process, a fiber of a polymer solution was continuously spun through a spinneret by a large electrostatic force to settle on a collector. The electrospun nanofibers have some advantages like good connection of pores, high specific area and the probability to combine active ingredients on a nanoscale [7, 8].

Several factors such as solution concentration, solvent type, applied voltage, flow rate, and distance between syringe tip and collector play a significant role in the morphological characteristics of produced fibers [9, 10, 11].

Polyamide-6 (PA-6) or polycaprolactam is a biodegradable and synthetic polymeric substance with good physical and mechanical properties [12, 13]. PA-6 nano or microfibers have wide demands in the textile industry. In recent years, researchers have paid attention to correction of nylon-6 nanofibers by several compounds. For example, Ding, *et al.* [14] observed a morphology between main fibers of electrospun PA-6 looking like spider web. They found that this morphology could be formed by adding different inorganic salts as well as applied voltage and other electrospinning parameters.

Propolis is a natural gummy substance derived from honey bees from different plant sources. Therefore, propolis can contain a complex mixture of chemicals such as resins (50%), combination of phenolic acids and flavonoids, waxes (about 30%), essential oils (10%), pollen (5%) and several organic compounds (5%), vitamins (B groups), fatty acids, saccharides, ketones, esters, steroids and quinones [15, 16, 17].

Because of some properties of propolis such as antioxidant and antimicrobial, many researches have been conducted to use it [18, 19, 20, 21, 22]. There are some research projects on incorporation of propolis into polymeric films [16]; however, a limited number of publications on electrospinning applications of propolis are available. Pastor, *et al.* [6] prepared edible films by mixing hydroxypropylmethylcellulose (HPMC) with various concentrations of propolis ethanolic extract so that he could evaluate the films antifungal activity against *Aspergillus niger* and *Penicillium italicum*. Erdem, *et al.* [6] fabricated propolis extract-blended polyurethane base nanofibers by electrospinning technique especially for wound dressing applications. They studied the morphological characteristics of polyurethane (PU)/propolis blended electrospun nanofibers. Kim, *et al.* [23] fabricated propolis/PU mixed nanofibers using electrospinning of the solution. They found the blended nanofibers becoming point-bonded with increasing propolis in the mixture.

* Corresponding author.
E-mail addresses: m.razavizadeh@rifst.ac.ir, bmrz110@gmail.com (B.M. Razavizadeh).

https://doi.org/10.1016/j.heliyon.2020.e04784
Received 20 December 2019; Received in revised form 21 July 2020; Accepted 20 August 2020

Asawahame, *et al.* [5] utilized propolis in Polyvinyl pyrrolidone (PVP) and also polyvinyl alcohol (PVA) applying electrospinning method. They concluded that incorporation of 2% w/v propolis in 8%–10% w/v PVP K90 nanospun fibers led to smooth and identical fiber morphology which dissolved quickly in water within 10 s. Sutjarittangtham, *et al.* [24] incorporated different concentrations of propolis ethanolic extract in nanofibers of polycaprolactone (PCL) applying electrospinning process and investigated their morphology by SEM and the functional group by FT-IR.

Although many studies have been carried out on the properties of various polymers such as PCL, PU, PVP, and ... mixed with propolis [25, 26], no study has been seen by the authors focusing on the blending of PA-6 polymer with propolis extract; moreover, the question is, how much of the PA-6 polymeric properties is affected by the propolis extract in the blended matrix. Therefore, the objective of this study was to investigate the antioxidant activity, and also the characteristics of electrospun PA-6 polymer fibers blended with different concentrations of propolis extract. Accordingly, the effects of different concentrations of PA-6 solution in formic acid (as solvent) as well as the addition of EEP to these solutions were investigated regarding thermal and morphological characteristics of the fibers using filed emission scanning electron microscopy (FESEM), thermal analyses (TGA and DSC), X-ray diffraction (XRD) patterns, and Fourier Transform Infrared Spectroscopy (FTIR) techniques.

2. Material and methods

2.1. Materials

Polyamide- 6 (PA-6, M_w = 17,000 Da), and Ethanol (96%) were purchased from market in Iran. Formic acid (98%) was purchased from Merck chemical Co. Propolis was obtained from around Mashhad (Iran).

2.2. Methods

Propolis Ethanolic extract (EEP) was obtained having mixed crude propolis 30% (w/v) in ethanol- 70% at room temperature under continuous stirring for 24 h. The suspension was filtered by Wathman filter paper (No. 1) twice. The supernatant was dried in a dark place and at the room temperature. The dried extracts were stored for further uses in dark glass containers and in the refrigerator [27].

2.3. Preparation of polymeric solutions

In this article two systems are studied. The first includes various concentration of PA-6 in formic acid. The second contains EEP and PA-6 in formic acid. The PA-6 solutions of 25, 30, 35, and 40% (w/v) were made by dissolving proportional amount of polymer in formic acid (98%) while they were stirred on the magnetic stirrer at 50–60 °C for about 2 h. After the solutions were made, they were cooled to reach room temperature. In the case of PA-6 solution (35%) after cooling, appropriate amounts of EEP (with a ratio 20, 30, 40, and 50 % by weight respect to polymer) were added to the polymer solution. All prepared solutions were used for further measurements and electrospinning [28, 29].

The viscosities of polymer solutions were measured using rotary viscometer (Bohlin Model Visco 88; Malvern Instruments Ltd., England) with C4 spindle, equipped with rotary heating system (Julabo, Germany. F12-MC: Julabo Labor Technik). Viscosity values were read at a shear rate of 61 s^{-1} for all solutions [30].

The electrical conductivities of polymer solutions were measured with a portable digital laboratory conductivity meter (PT. Prolabms Murni Swadaya, RS232 Conductivity Mater, 8302, Indonesia) at ambient temperature [12].

2.4. Electrospinning procedure

Electrospinning process was performed in a full automatic electrospinning unit (ANSTCO-RN/X model, Asia Nano-Structure Company, Iran). The polymer solution was carried in a plastic syringe (10 ml) and then was sent to the collector plate covered with aluminum foil (6 cm × 6 cm) through a plastic tube (VYGON, France) connected to a steel nozzle (Gauge 18, Sigma - Aldrich) at the end. Electrospinning of PA-6 or PA-6/EEP blended solutions were carried out at voltage: 25 kV, flow rate: 0.5 ml h^{-1}, distance of tip to collector: 15 cm. Electrospinning of all polymer solutions were made in a close chamber for 1 h. At the time of the procedure, temperature and relative humidity were in the range of 25–30 °C and 30–35% RH, respectively [12, 31].

2.5. Fiber characterization

2.5.1. Thermal analysis of fiber mats

Thermal gravimetric analysis (TGA) was performed to assess the fibers rotting and to reduce the sample mass as a function of temperature which was in accordance with ASTM E1131-14 standard using TGA device (Mettler Toledo, Model TGA/DSC1, Switzerland). Under N_2 atmosphere, the samples were heated from 25 to 600 °C with 10 °*C min*$^{-1}$ in rate.

Differential scanning calorimeter (DSC) was used for measuring the melting enthalpy (ΔH_m), and the melting temperature (T_m) of electrospun PA-6/EEP fibers on a DSC apparatus (METTLER TOLEDO، Model DSC100- L, Switzerland). In these experiments, the samples were heated under N_2 atmosphere from 25 to 300 °C with the rate of 10 °C min^{-1} [32]. From DSC data, the crystallinities (Xc) of the fibers were determined from Eq. (1):

$$Xc\ (\%) = (\Delta H_m)/\ \Delta H_{0m}) \times 100 \quad (1)$$

Where ΔH_m and ΔH_{0m} are the heats of melting for PA-6/EEP polymer samples and PA-6 in full crystalline state, respectively; where the amount of ΔH_{0m} is equal 230 Jg^{-1} [33].

2.5.2. FTIR analysis

FTIR spectra of PA-6 and PA-6/EEP fiber mats and also for EEP were obtained using a probe spectrophotometer (ALPHA, ATR Eco, Bruker, Germany) as 16 scans in a range of wavelength of 400–4000 cm^{-1} with 2 cm^{-1} resolution. FTIR spectrum software was applied to convert files into numerical data and analyze them [34].

2.5.3. FESEM studies

The microstructure of electrospun fibers was studied using FESEM (TESCAN Co., Model: MIRA3, Czech Republic) at 15 kV voltage. The distribution of fibers diameters was calculated by the Image J software from FESEM images [34].

2.5.4. XRD patterns

The electrospun fiber mats were subjected to XRD instrument (Unisantis, Model: XMD 300, Germany) at a current 0.7 A and a voltage 40 kV and 0.1541 nm wavelength of X-ray radiation [35].

2.6. Evaluation of EEP release from fibers

About 15 mg of the EEP/PA-6 electrospun fiber mats were weighed and immersed into a glass flask containing 40 mL ethanol (96%) medium under magnetic stirring (100 rpm) at 25 °C [36]. At intervals, 1 mL of supernatant was periodically taken and total phenolic extract and also DPPH radical scavenging of the fibers were evaluated.

The released total phenolic amounts of the fibers were evaluated according to the Folin-Ciocaltue method [37]. 100 μL of aliquot each sample was taken into tubes containing 6 mL water. 500 μL Folin-Ciocaltue reagent was added to each tube. After 10 min, sodium carbonate solution (20 %w/v) was added to each of them and they were incubated at room temperature for 90 min in a dark space. The absorbance of samples was measured by UV–Vis spectrophotometer (Hach, DR5000, USA) at 760 nm. The standard curve was obtained for 0–900 ppm of Gallic acid as internal reference. Total phenolic compounds were illustrated as microgram Gallic acid equivalent per 1 g of the fiber mat.

The antioxidant activity for the fibers was evaluated via 2, 2-diphenyl-1-picrylhydrazyl (DPPH) free radical scavenging assay [36]. Three mL of 0.1 mM DPPH ethanolic solution was added to 200 μL of the aliquot each sample. The mixtures were placed in dark space for 30 min at 25 °C. The absorbance of the solutions was read at 517 nm using UV–Vis spectrophotometer (Hach, DR5000, USA). The DPPH ethanolic solution without fiber was used as the control. The antioxidant activity (%) was computed as Eq. (2):

$$\text{Antioxidant Activity } (\%) = 100 \times \left(1 - \frac{A_s}{A_c}\right) \quad (2)$$

where A_s and A_c are the absorbance of the sample solution and the control solution, respectively.

2.7. Statistical data analysis

Data analysis was conducted on a completely randomized design with Minitab software (version 4. 2. 16). The meanings were compared using Tukey test at a level of 95% confidence ($P < 0.05$). The graphs were drawn using Excel 2013 software. In this research all tests were performed in three replications.

3. Results and discussion

3.1. Polymer solutions properties

Electrical conductivity and apparent viscosity of PA-6 and EEP/PA-6 solutions were evaluated and the results were presented in Table 1. The viscosities of the PA-6 solutions increased with more polyamide dissolving in formic acid from 25% to 40% (w/v). Meanwhile, the conductivity values were relatively decreased for PA-6 solutions. These observations can be caused by the increased molecular entanglements [29].

According to the results in Table 1, the viscosity decreased partly with increasing EEP in (35%) PA-6 solution up to 40% EEP and then increased significantly for 50% EEP. These results could be attributed to less chain entanglements occurring between the molecules [29]. On the other hand, the conductivities of PA-6/EEP solutions decreased slightly with increasing of EEP amounts. This trend can be ascribed to the decreasing ionic strength and increasing EEP amount in polymer solution.

3.2. Characterizes of fibers

3.2.1. Morphology of fibers

Fiber size distributions for both PA-6 and EEP/PA-6 systems were calculated by image J software from FESEM images. The FESEM images of the electrospun fibers of PA-6 with different concentration in formic acid have been presented in Figure 1. As can be seen, the FESEM images indicate that the randomly oriented electrospun fibers showed smooth surface with almost the same diameters along their lengths in the strip as well as lacking any beads According to Figure 2a-d, the size distribution of PA-6 fibers has been placed in the range of 100 nm–1500 nm. In the solution of PA-6 25% in formic acid, there is a partial fiber less than 100 nm (about 4%) and most of the size distribution of main fibers was in the range of 300–500 nm (Figure 1a). With increasing PA-6 in the solvent, the viscosity of the solution increased while the conductivity decreased (Table 1). Increasing the viscosity of these solutions occurred due to the increasing molecular weight (concentration) of the dissolved PA-6 polymer as well as increasing molecular entanglements [29]. On the other hand, decreasing the conductivity caused the jet to stretch less, which led to forming wider diameter fibers [38, 39]. Therefore, these properties can control the solution flow rate through the capillary [40] and that in turn affects the size distribution of electrospun fibers and leads them to shift to the left, that is to say that the fibers became broader or the fiber diameter increased.

The FESEM images of the EEP/PA-6 blended electrospun fibers mats were shown in Figure 3. Similar to PA-6 electrospun fibers, the blended electrospun fibers of EEP/PA-6 were exhibited through randomly oriented fibers and in the strip form without any beads. Also, the FESEM images obtained from fiber mats contained high concentrations of EEP in the polymer blend (40% and 50%) indicate that some fibers were merged or bonded together (Figure 3c-d). This was especially evident in the concentration of 50% of EEP. This morphology can be illustrated by the low volatility of EEP and larger viscosity of EEP/PA-6 solution. Therefore, it becomes increasingly difficult for electrospun material to dry completely before being taken to a collector. In addition, the adhesive property of EEP can provide the connection of fibers with each other at their crossing points [2].

Table 1. Conductivity and viscosity of PA-6 and EEP/PA-6 polymer solutions in formic acid and Mean diameter of the resulting electrospun fibers (Mean ± SD).

Polymer solution (in acid formic)	Concentration (%)	Viscosity (Pa.s)	Conductivity (mS cm^{-1})	Mean Diameter (nm)
‡PA- 6	0	-	†0.51 ± 0.005^{d}	-
	25	5.5 ± 0.0^{c}	4.39 ± 0.005^{a}	487.7 ± 8.1^{c}
	30	8.7 ± 0.0^{b}	4.38 ± 0^{a}	577.3 ± 32.5^{b}
	35	17.7 ± 0.3^{a}	4.0 ± 0.221^{b}	625.0 ± 8.9^{ab}
	40	18.5 ± 0.3^{a}	3.70 ± 0.035^{c}	682.7 ± 45.4^{a}
§EEP/PA-6 (35%)	0	17.7 ± 0.3^{B}	4.0 ± 0.221^{A}	625.0 ± 8.9^{D}
	20	15.3 ± 0.7^{BC}	2.93 ± 0.20^{B}	943.3 ± 33.3^{C}
	30	13.45 ± 0.7^{C}	2.88 ± 0.19^{B}	1298.3 ± 24.5^{B}
	40	13.75 ± 0.2^{C}	2.76 ± 0.16^{BC}	1702.7 ± 43.5^{A}
	50	21.25 ± 1.6^{A}	2.51 ± 0.11^{BC}	1773.7 ± 7.5^{A}

*Different letters in each column (polymer solutions were analyzed separately: Lowercase letter for PA-6 and Capital letters for EEP/PA-6 polymer solutions) represent a meaningfull difference according the Tukey test at the level of 95% confidence ($P < 0.05$).

† Formic acid conductivity.

‡ Concentration is (w/v %).

§ Concentration is (w/w %).

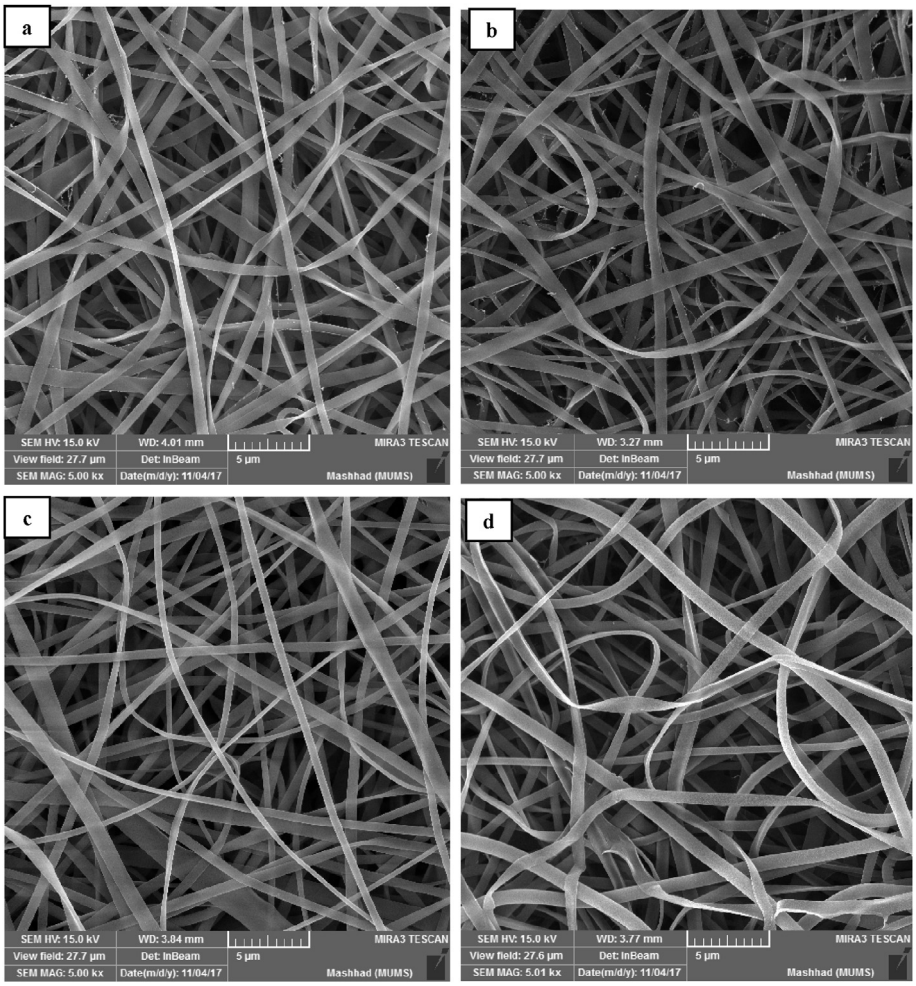

Figure 1. FESEM images of electrospun fibers of PA-6 with different concentrations (a) 25 (%w/v), (b) 30 (%w/v), (c) 35 (%w/v), (d) 40 (%w/v).

In the blended electrospun fiber mats of EEP/PA-6 solution (35%), minimum size of electrospun fibers started from about 300 nm in the case of (20%) EEP and the most population in size distribution of its electrospun fibers is 700–900 nm (Figure 4). While, with increasing the amount of EEP in (35 %) PA-6 solution the population of size distribution shifted to larger amounts of diameter. That is, increasing EEP in the polymer blend caused the number of broader strips to become more than narrow strips. These observations can be due to decreasing conductivity of EEP/PA-6 solutions with increasing EEP concentration as well as adhesion and low volatility of EEP [6].

Mean diameter of the electrospun fibers of PA-6 and EEP/PA-6 systems which were calculated using the ImageJ software are presented in Table 1. For PA-6 System, the mean diameter of electrospun fibers increased from 487 nm to 682 nm with increasing PA-6 concentration from 25% to 40%, respectively. Except for 25% PA-6 in formic acid, these changes were not significant together. Furthermore, the electrospun fiber diameters increased significantly ($p < 0.05$) (except between 40 and 50% of EEP) with increasing EEP concentrations in the PA-6 solution (35%) from 625 nm for 0% EEP to 1773 nm for 50% EEP, the fiber diameter was observed to be larger at 50% EEP concentration.

Chowdhury *et al.* [12] investigated electrospinning of polyamide-6 solutions in formic acid at various concentrations of 10–25%. They have found that increasing the concentration of polyamide in the solution leads to increasing viscosity and fiber diameter as well as decreasing conductivity. They showed that the concentration of the solution affects the morphology of the fiber such that beads are formed in the polyamide with concentrations less than 20%, while in higher concentrations the number of beads decreases. They ascribed this to the quick evaporation of the solvent from the jet surface because it is slower at lower concentration of solvent evaporation from the time the fiber reaches the aggregate surface.

The formation of some high aspect ratio nanofiber bounded in between the major fibers could be observed (in the dotted circles) in figure 5(a-b) for PA-6 25 % and 30 % systems, respectively. In these systems, high aspect ratio fibers were bounded with major fibers but not strongly. Also, some flakes were observed within the main fibers (as solid circles in Figure 5(a-b) in some places owing to the incomplete evaporation of solution [41]. While mean, for PA-6 35 % and 40 % systems, rarely some flakes could be seen in the solid circles in Figure 5(c-d), respectively. The electrospun fibers of EEP/PA-6 were free of high aspect ratio nanofibers or any flakes. Some researchers have reported such observations in electrospun nanofiber polyamide systems [42]. Nirmala, *et al.* [41] attributed these observations to formation of polyelectrolytic forms of PA-6 in formic acid and little ionization of amide groups in the polymer chains. Therefore, electrospinning of polymer in polar solvents leads to formation of smaller fiber diameter. Accordingly, the addition of nonionic EEP to PA-6 causes the ionization of amide groups to decrease as well as to lack high aspect ratio nanofibers or flacks.

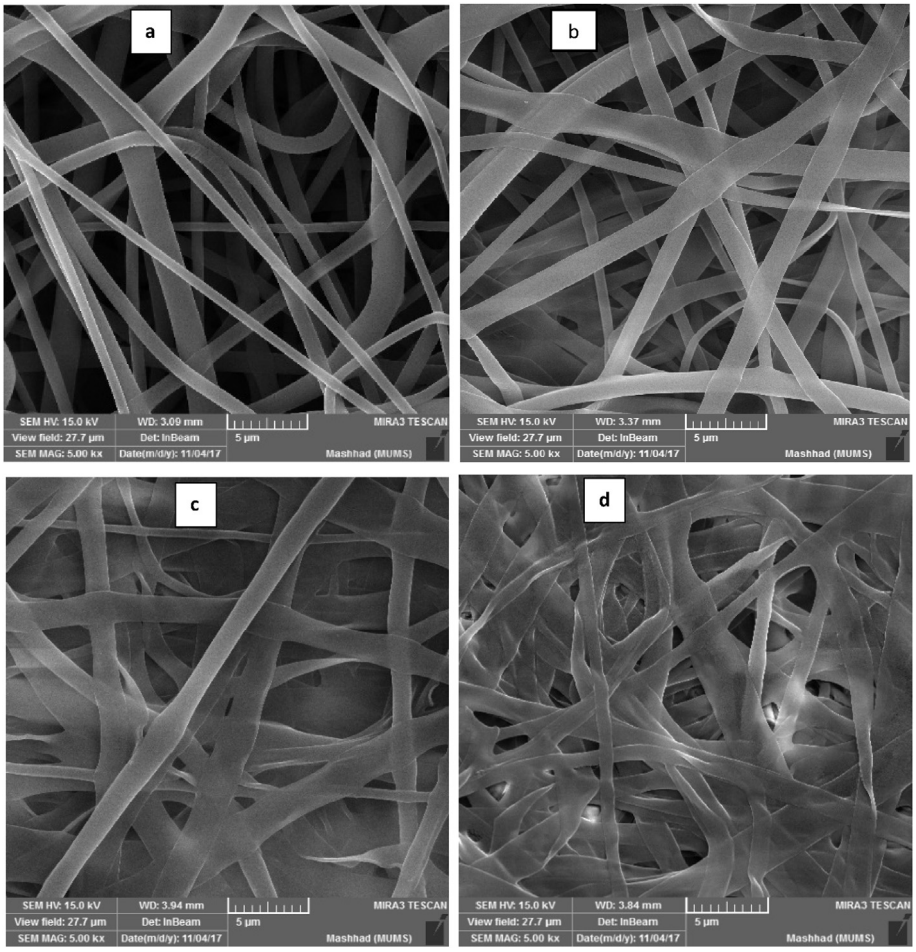

Figure 2. FESEM images of electrospun fibers of PA-6 (35 w/v %) blended with different concentrations of EEP: (a) 20 (%w/v), (b) 30 (%w/v), (c) 40 (%w/v), (d) 50 (%w/v).

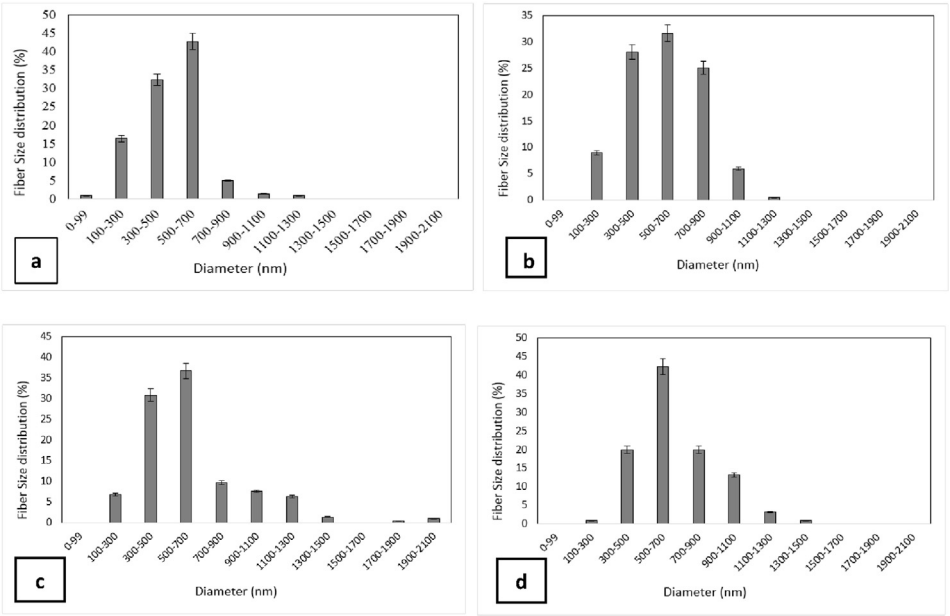

Figure 3. Size distribution of electrospun fibers of PA-6 with different concentrations: (a) 25 (%w/v), (b) 30 (%w/v), (c) 35 (%w/v), (d) 40 (%w/v) in formic acid.

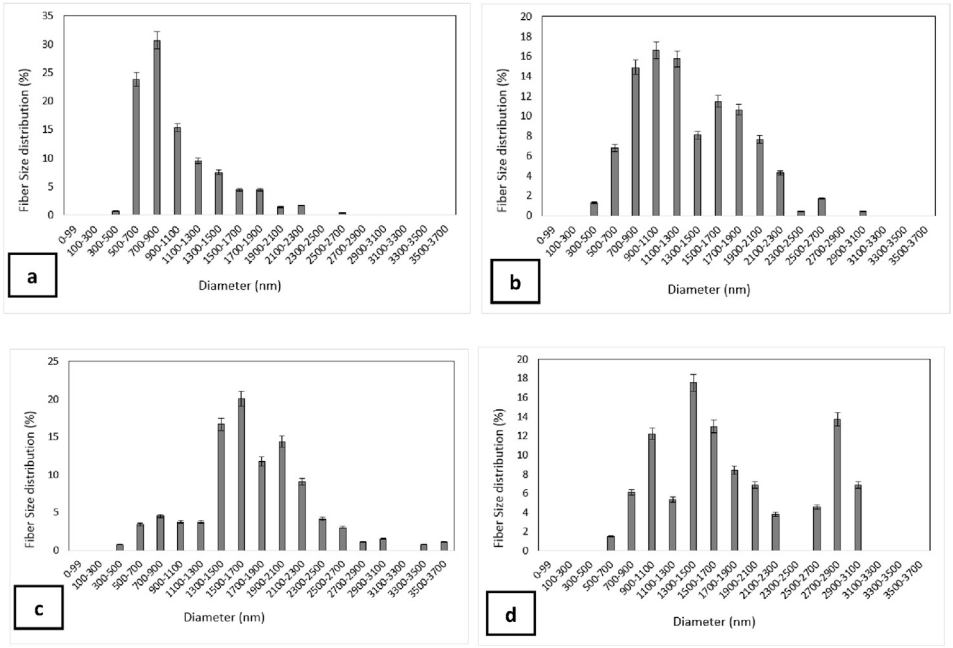

Figure 4. Size distribution of electrospun fibers of PA-6 blended with different concentrations of EEP: (a) 20 (%w/v), (b) 30 (%w/v), (c) 40 (%w/v), (d) 50 (%w/v).

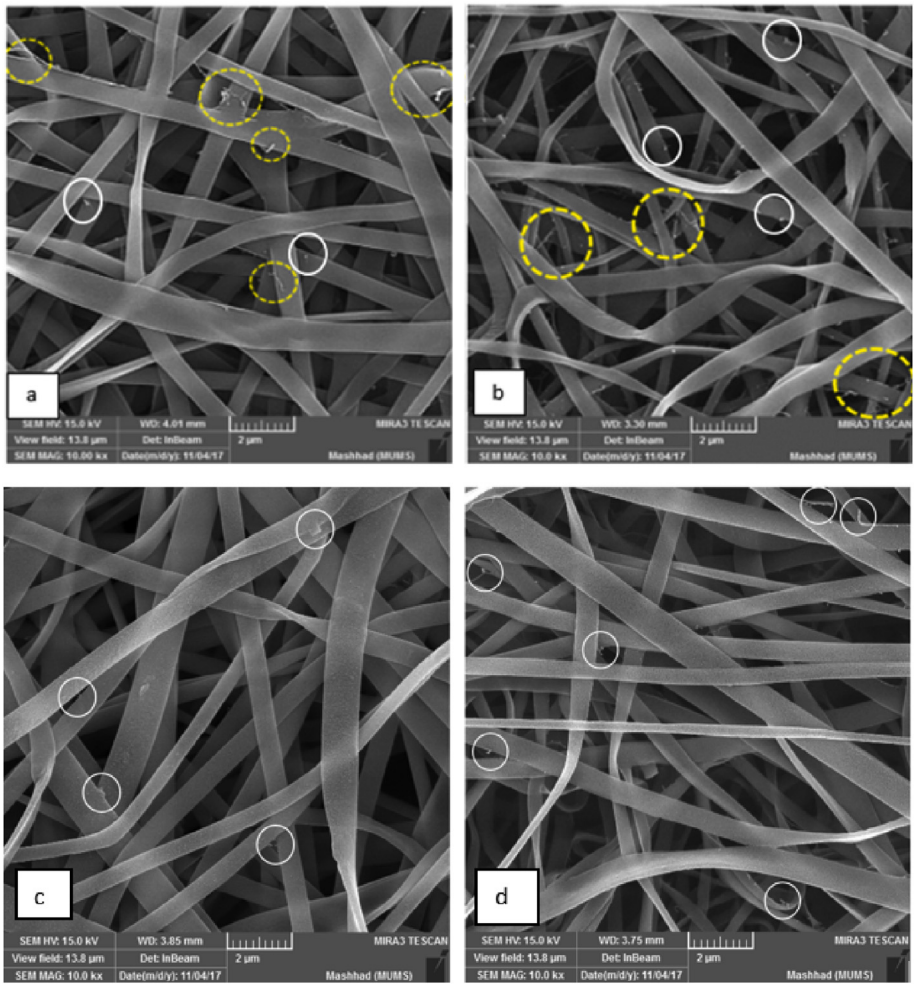

Figure 5. FESEM images of electrospun fibers of various concentrations of PA-6 in formic acid: (a) 25 %, (b) 30 %, (c) 35%, and (d) 40 %. Dotted circles indicate the high aspect ratio nanofibers and solid circles indicate the defective fibers or flakes (magnification 10 kx).

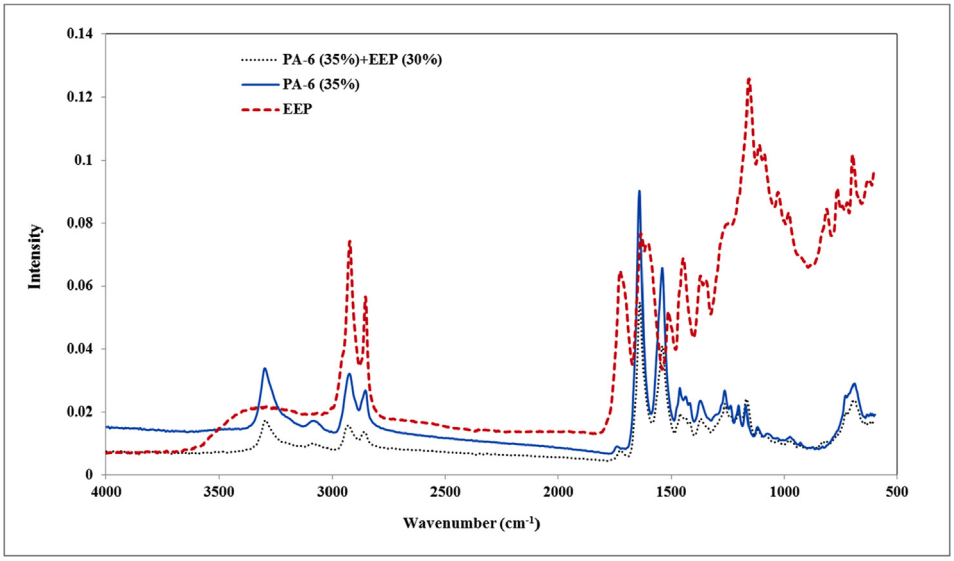

Figure 6. FTIR spectra of EEP, electrospun fibers of the PA-6 (35 % w/v) and blended PA-6 (35%w/v)/EEP (30% w/w).

3.2.2. FTIR studies

The Fourier transformation infrared spectrum of EEP, the PA-6 (35%) and electrospun blende fibers of EEP (30%) in PA-6 (35%) were shown in Figure 6. For EEP spectrum, a broad band appeared at wave number of 3344 cm^{-1} represented to OH groups (such as phenolic compounds) in EEP. Also, strong peaks in wavenumbers 2914 cm^{-1} and 2851 cm^{-1} show the stretching of CH_2 group which were asymmetric and symmetric, respectively. A band at 1724 cm^{-1} is probably related to stretching vibration of carboxyl (-COOH) groups, two bands at 1633 cm^{-1} and 1602 cm^{-1} could be attributed to stretching vibration of C=C groups and or C=O groups due to amino acids and flavonoids. The band at 1512 cm^{-1} are potentially related to aromatic ring deformations C=C stretching and at 1446 cm^{-1} for CH bending and aromatic stretching vibrations, or OH bending [43].

The significant peak in the polyamide sample without EEP (i.e. PA-6) in the wavenumbers of 3299 cm^{-1} was related to the amine (NH) groups [44], which was also present in the blend of EEP/PA-6 fiber mat, but this peak was not observed in EEP. The peaks of the region, 2924 cm^{-1} and 2853 cm^{-1}, were considered to belong to the stretching of methylene (CH_2) and methyl (CH_3) groups and a peak of 1640 cm^{-1} was for stretching of carbonyl group (C = O) [45, 46]. Similar Spectrum was observed for the blended fibers containing PA-6 and EEP in compared with PA-6 fibers. Overall, the FTIR spectrums of both PA-6 and EEP/PA-6 electrospun fibers are very similar. However, the peak intensities in blend fibers decreased comparing PA-6 fibers. It seems that introducing EEP to the PA-6 solution caused a partially shifting just about 1–4 cm^{-1} in FTIR spectrum. Due to the lack of appearance of new peaks compared to PA-6, it sounds that there are no new bonds. It revealed that there was a weak interaction between the components and most probably, propolis was distributed throughout the PA-6 polymer matrix. Similar results were reported by Kim and his team for electrospun propolis/polyurethane composite nanofibers, as they claimed there was a homogenous distribution of the propolis in the PU matrix [23].

Supaphol *et al.* [47] studied the properties of polyamide fibers through their FTIR spectra in various solvents. They concluded that the properties of electrospun fibers depend on the solvent-solvent properties. Moreover, Stephens *et al.* [47, 48] concluded that the polyamide has specific conformations that can transfer to another one under electric field during electrospinning. These transfers occur in the regions of 1443, 1470, and 1480 cm^{-1}.

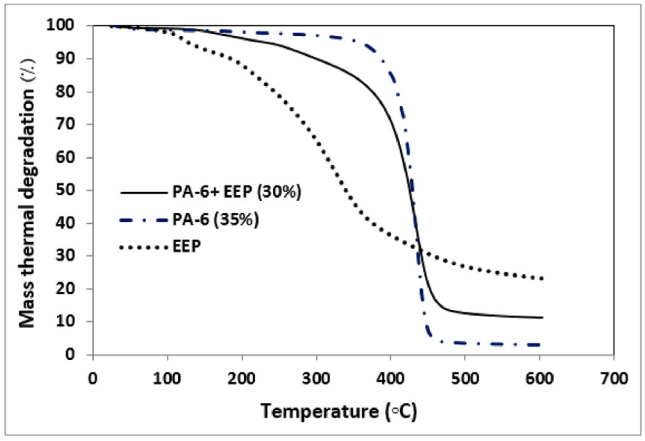

Figure 7. TGA thermo grams of EEP, electrospun fibers of polyamide PA-6, and blended of EEP (30% w/w)/PA-6 (35% w/v).

3.2.3. Thermal analysis

The TGA thermograms (thermal mass degradation) of EEP, polyamide PA-6 fiber, and PA-6 fiber containing 30% EEP are shown in Figure 7. Obviously, EEP degradation started from nearly 100 °C, while, the weight loss of PA-6 started from about 350 °C and it was almost completely degraded at 450 °C. However, for the EEP/PA-6 system thermal degradation began around the temperatures of 200 °C and completed at 450 °C. Thermal degradation changes are clearly visible for these systems. Having considered the differences in TGA thermograms of EEP/PA-6 electrospun fiber in comparison with PA-6 and EEP, it can be concluded that mixture of PA-6 and EEP is a simple one, not involving very complex interactions.

The DSC analyses of EEP, and PA-6 electrospun fiber mats containing different concentrations of EEP were done. The results within the range of 0–300 °C temperatures indicated the endothermic process for EEP/PA-6 fiber mats, while for EEP there were not any considerable changes. In all samples of EEP/PA-6 fiber mats, there was an endothermic peak in the range of 170–250 °C which is related to the melting point of samples. The addition of EEP to polymer matrix did not lead to the formation of more endothermic peaks, which indicates the miscibility of EEP and PA-6 [49]. The melting temperature (T_m), enthalpy of melting (ΔH_m) and crystallinity percentages (Xc) of EEP/PA-6 fiber mats from DSC measurements were specified in Table 2. For EEP/PA-6 electrospun fiber mats, T_m were obtained in the range of 215.8–223.2 °C. Accordingly, T_m, ΔH_m, as well as Xc decreased with the increasing of EEP in the PA-6 electrospun fibers.

Table 2. DSC data analyses of EEP/PA-6 electrospun fibers at different concentrations of EEP.

EEP concentration (%) in EEP/PA-6 fiber	T_m (°C)	ΔH_m (J/g)	Xc (%)
0	223.2	96.621	41.99
20	218.3	62.322	27.08
30	218.3	39.736	17.27
40	215.2	40.002	17.38
50	215.8	37.663	16.37

The greatest effect on melting enthalpy as well as the reduction of melting temperature and crystallinity was observed in 20% EEP concentration. While higher concentrations of EEP do not exert significant changes in thermal characteristics compared by 20% EEP in fiber samples. The small variations in thermal temperatures can indicate weak interactions between EEP and PA-6 in blend fibers.

As Tables 1 and 2 depict, increasing the concentration of EEP in the blended PA-6 fibers, not only increased the mean diameter of the fibers, but also it decreased the melting point and percentage of crystallinity. These results can be considered in connection with the rapid solidification of the stretched EEP/PA-6 blended polymer chains, which can limit the crystallization development and increase the diameter of the fibers [40, 50].

For more focus on crystallinity of the fibers, the X-ray patterns of the polymer systems were studied. Figure 8 shows the X-ray patterns of (PA-6 (35%) and (30%) EEP/PA-6) polymer systems. The patterns refer to the broad band polyamide fibers, which indicate the amorphous structure for both of the systems. In addition, the presence of these bands in the same region is due to the similarity of the polymer PA-6 and PA-6/EEP structures, which did not change significantly by the presence of EEP. Marsano *et al.* [40] studied the properties of electrospinning of polyamide solutions and also the resulting fibers and concluded that the melting temperature was independent of the concentration, voltage and relative humidity of the medium. They found that the rapid solidification in electrospinning process can limit the development of crystallinity because the macromolecular chains did not have enough time to make crystalline forms.

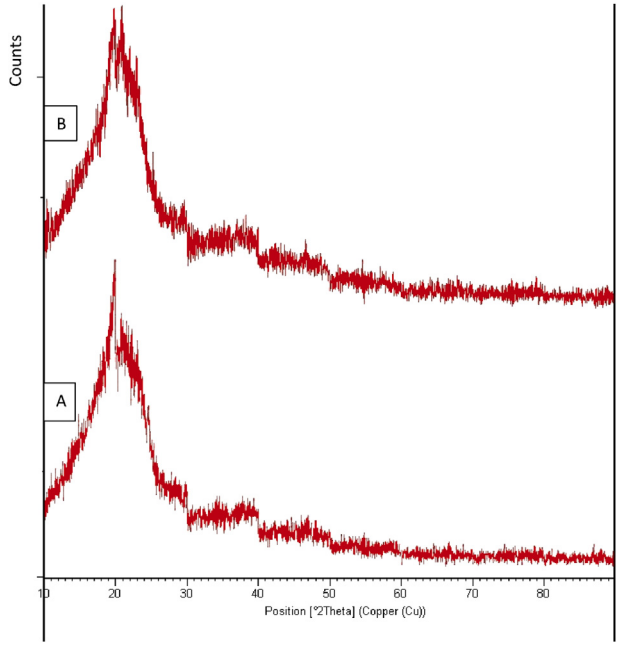

Figure 8. XRD patterns of electrospun fibers: (A) polyamide PA-6 and (B) blended of EEP (30% w/w)/PA-6 (35% w/v).

3.3. Evaluating antioxidant activity of EEP/PA-6 fibers

The antioxidant activity of a compound is mainly dependent on their oxidizing-reducing properties, which can play a crucial role in neutralizing free radicals, deactivating single oxygen, or peroxide decomposition. Typically, the antioxidant capacity depends on the total amount of phenolic compounds and not only they have a linear relationship together, but also the variety of phenolic and flavonoid compounds cause differences in antioxidant activity [51].

In order to evaluate quantification of the antioxidant activity of the fibers directly, the release studies of the propolis total phenolic compounds were performed. The amount of released total phenolic compounds from the (EEP/PA-6) electrospun fiber mats were plotted at different time intervals within 300 min as shown in Figure 9a. Initially the amounts of released compounds gradually increased and reached a steady rate after about 1 h. The released total phenolic compounds from the mats increased with increasing EEP concentration. The maximum amounts of extraction of these compounds were reported at 45th minute, including 170, 185, 207, 212 μg/g of the fiber mats for 20%, 30%, 40% and 50% of EEP concentrations, respectively. On the other hand, the antioxidant activities of the mats were drawn at different time intervals in Figure 9b. The antioxidant activity of the fiber increased with increasing the percentage of EEP in the EEP/PA-6 electrospun fibers, which seems to depend on the concentration of total phenolic compounds release. As it can be observed, the maximum antioxidant activity (about 57.5%) was obtained for the mats containing 50% EEP at 45th minute. For the EEP concentrations 20%, 30%, and 40% in this time, the antioxidant activities were reported 48.9%, 49.3%, 53.9%, respectively. The low antioxidant activity of these fibers can be ascribed to the low content of phenolic compounds in propolis [52]. Kumazave *et al.* [51] investigated antioxidant activity of different propolis samples with various geographic origins. They correlated this property with the total phenolic and flavonoid amounts. They reached the conclusion that DPPH free radical scavenging activity for some propolis samples, with more

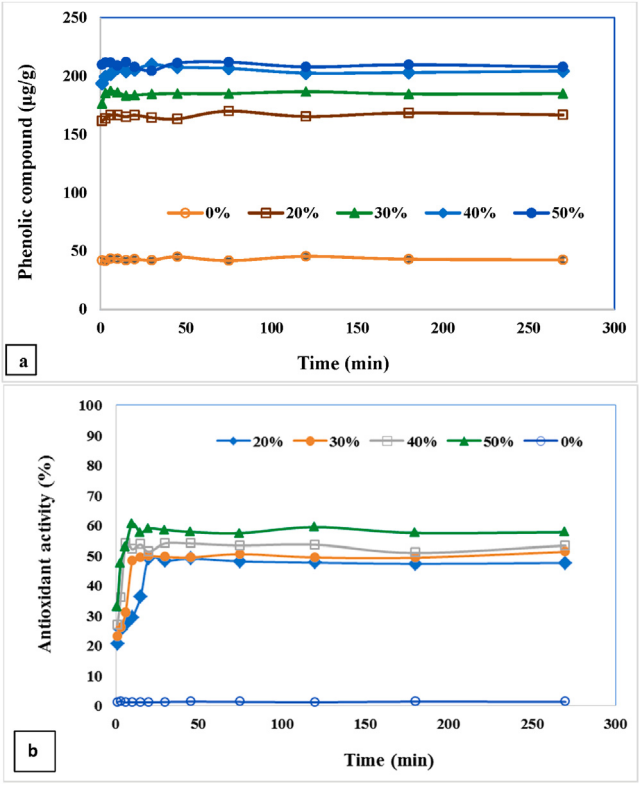

Figure 9. The released total phenolic compounds (a) and antioxidant activity (b) of the PA-6/EEP electrospun fibers against time.

polyphenol content, reached over 95%. Also, Sutjarittangtham, *et al.* [53] studied the preparation of the loaded propolis extract with different concentrations (0–10% w/v) in polylacticacid (PLA) nanofiber mats by electrospinning technique. They concluded that the amount of total phenolic and flavonoid contents in propolis had a synergic effect on the antimicrobial as well as antioxidant properties of nanofibers.

On the other hand, Mascheroni *et al.* [54] incorporated propolis in the biopolymer modified PLA to prepare a delivery procedure for food packaging purposes. They studied release kinetic of the polyphenols from improved PLA/propolis film in water medium as a function of time and found that their delivery procedure could be an efficient one for direct contact with aqueous media because of polyphenols acids release in suitable amount in the food whereas the flavonoids would stay in the polymer to function at the interface of polymer-food. In the present study, the results showed the release rate in ethanol medium is relatively fast in the first 20 min. Therefore, the PA-6/EEP fiber mats can be convenient for fatty medium foods.

4. Conclusion

Incorporation of propolis ethanolic extract with different concentrations in the PA-6 electrospun fiber mats were investigated. The morphological studies indicated that the EEP/PA-6 blending fibers, in contrast with PA-6 systems, did not contain any high aspect ratio nanofibers as also the diameter fibers increased as the EEP concentration increased. FTIR spectrums and thermal properties exhibited the simple mixtures of PA-6 and EEP in blend fibers which did not involve very complex interactions. On the other hand, interpolation of propolis in the PA-6 fiber mats could supply antioxidant fiber mats. According to the results, these blended fibers have potentials to be applied in medicine and food industries.

Declarations

Author contribution statement

Bibi M. Razavizadeh: Conceived and designed the experiments; Performed the experiments; Analyzed and interpreted the data; Contributed reagents, materials, analysis tools or data; Wrote the paper.

Razieh Niazmand: Conceived and designed the experiments; Analyzed and interpreted the data.

Funding statement

This research did not receive any specific grant from funding agencies in the public, commercial, or not-for-profit sectors.

Competing interest statement

The authors declare no conflict of interest.

Additional information

No additional information is available for this paper.

References

[1] R.U.İ. Erdem, E. Sancak, D. Kocak, M. Akalin, Effect of propolis extract to morphology of electrospun polyurethane nanofibers, Nanostruct. Mater. 7 (2013) 21–26.

[2] C. Pastor, L. Sánchez-González, M. Cháfer, A. Chiralt, C. González-Martínez, Physical and antifungal properties of hydroxypropylmethylcellulose based films containing propolis as affected by moisture content, Carbohydr. Polym. 82 (4) (2010) 1174–1183.

[3] Z. Chu, T. Zhao, L. Li, J. Fan, Y. Qin, Characterization of antimicrobial poly (Lactic Acid)/nano-composite films with silver and zinc oxide nanoparticles, Materials (Basel, Switzerland) 10 (6) (2017).

[4] P. Upasani, T.V. Sreekumar, V.G. Gaikar, N. Jha, Preparation of ZnO nanoribbon–MWCNT composite film and its application as antimicrobial bandage, antibacterial filter and thermal IR camouflage material, Bull. Mater. Sci. 40 (4) (2017) 865–876.

[5] C. Asawahame, K. Sutjarittangtham, S. Eitssayeam, Y. Tragoolpua, B. Sirithunyalug, J. Sirithunyalug, Formation of orally fast dissolving fibers containing propolis by electrospinning technique, Chiang Mai J. Sci. 42 (2) (2015) 469–480.

[6] A. Baji, Y.-W. Mai, S.-C. Wong, M. Abtahi, P. Chen, Electrospinning of polymer nanofibers: effects on oriented morphology, structures and tensile properties, Compos. Sci. Technol. 70 (5) (2010) 703–718.

[7] S. Thenmozhi, N. Dharmaraj, K. Kadirvelu, H.Y. Kim, Electrospun nanofibers: new generation materials for advanced applications, Mater. Sci. Eng. 217 (2017) 36–48.

[8] M. Mirjalili, S. Zohoori, Review for application of electrospinning and electrospun nanofibers technology in textile industry, J. Nanostructer. Chem. 6 (3) (2016) 207–213.

[9] M. Naghibzadeh, M. Adabi, Evaluation of effective electrospinning parameters controlling gelatin nanofibers diameter via modelling artificial neural networks, Fibers Polym. 15 (4) (2014) 767–777.

[10] A. Haider, S. Haider, I.-K. Kang, A comprehensive review summarizing the effect of electrospinning parameters and potential applications of nanofibers in biomedical and biotechnology, Arabian J. Chem. 11 (2015) 1165–1188.

[11] S.S. Esnaashari, M. Naghibzadeh, M. Adabi, R. Faridi Majidi, Evaluation of the effective electrospinning parameters controlling Kefiran nanofibers diameter using modelling artificial neural networks, Nanomed. Res. J. 2 (4) (2017) 239–249.

[12] M. Chowdhury, G. Stylios, Effect of experimental parameters on the morphology of electrospun Nylon 6 fibres, Int. J. Basic Appl. Sci. 10 (2010) 70–78.

[13] R.A. da Paz, A.M. Damião Leite, E.M. Araújo, V. da Nóbrega Medeiros, T.J. Alves de Melo, L.A. Pessan, Mechanical and thermomechanical properties of polyamide 6/Brazilian organoclay nanocomposites, Polimeros 26 (1) (2016) 52–60.

[14] B. Ding, C. Li, Y. Miyauchi, O. Kuwaki, S. Shiratori, Formation of novel 2D polymer nanowebs via electrospinning, Nanotechnology 17 (15) (2006) 3685–3691.

[15] M.G. Miguel, S. Nunes, S.A. Dandlen, A.M. Cavaco, M.D. Antunes, Phenols and antioxidant activity of hydro-alcoholic extracts of propolis from Algarve, South of Portugal, Food Chem. Toxicol. 48 (12) (2010) 3418–3423.

[16] C. Juliano, C.L. Pala, M. Cossu, Preparation and characterisation of polymeric films containing propolis, J. Drug Deliv. Sci. Technol. 17 (3) (2007) 177–181.

[17] F.C. da Silva, C.S. Favaro-Trindade, S. Alencar, M. Thomazini, J. Balieiro, Physicochemical properties, antioxidant activity and stability of spray-dried propolis, J. ApiProduct ApiMed. Sci. 3 (2011) 94–100.

[18] L. Drago, B. Mombelli, E. De Vecchi, M.C. Fassina, L. Tocalli, M.R. Gismondo, In vitro antimicrobial activity of propolis dry extract, J. Chemother. 12 (5) (2000) 390–395.

[19] S. Stepanović, N. Antić, I. Dakić, M. Švabić-Vlahović, In vitro antimicrobial activity of propolis and synergism between propolis and antimicrobial drugs, Microbiol. Res. 158 (4) (2003) 353–357.

[20] F. Scazzocchio, F.D. D'Auria, D. Alessandrini, F. Pantanella, Multifactorial aspects of antimicrobial activity of propolis, Microbiol. Res. 161 (4) (2006) 327–333.

[21] C. Perez-Perez, C. Regalado-González, C.A. Rodríguez-Rodríguez, J.R. Barbosa-Rodríguez, F. Villaseñor-Ortega, Incorporation of antimicrobial agents in food packaging films and coatings, Adv. Agri. Food Biotechnol. (2006) 193–216. Research Signpost, Kerala, India.

[22] S. Hajinezhad, B.M. Razavizadeh, R. Niazmand, Study of antimicrobial and physicochemical properties of LDPE/propolis extruded films, Polym. Bull. 77 (8) (2020) 4335–4353.

[23] J.I. Kim, H.R. Pant, H.J. Sim, K.M. Lee, C.S. Kim, Electrospun propolis/polyurethane composite nanofibers for biomedical applications, Mater. Sci. Eng. 44 (Supplement C) (2014) 52–57.

[24] K. Sutjarittangtham, S. Sanpa, T. Tunkasiri, P. Rachtanapun, P. Chantawannakul, U. Intatha, K. Pengpat, G. Rujijanagul, S. Eitssayeam, Preparation of polycaprolactone/ethanolic extract propolis nanofibers films, Adv. Mater. Res. 506 (2012) 226–229.

[25] C.Y. Chao, M.P. Mani, S.K. Jaganathan, Engineering electrospun multicomponent polyurethane scaffolding platform comprising grapeseed oil and honey/propolis for bone tissue regeneration, PloS One 13 (10) (2018), e0205699.

[26] S. Jaganathan, M. Prasath Mani, A. Ismail, P. Prabhakaran, G. Nageswaran, Tailor-made multicomponent electrospun polyurethane nanofibrous composite scaffold comprising olive oil, honey, and propolis for bone tissue engineering, Polym. Compos. 40 (5) (2018).

[27] M. Popova, S. Silici, O. Kaftanoglu, V. Bankova, Antibacterial activity of Turkish propolis and its qualitative and quantitative chemical composition, Phytomedicine 12 (3) (2005) 221–228.

[28] C. Mit-uppatham, M. Nithitanakul, P. Supaphol, Effects of solution concentration, emitting electrode polarity, solvent type, and salt addition on electrospun polyamide-6 fibers: a preliminary report, Macromol. Symp. 216 (1) (2004) 293–300.

[29] C. Mit-uppatham, M. Nithitanakul, P. Supaphol, Ultrafine electrospun polyamide-6 fibers: effect of solution conditions on morphology and average fiber diameter, Macromol. Chem. Phys. 205 (17) (2004) 2327–2338.

[30] F. Behrouzian, S.M.A. Razavi, H. Karazhiyan, The effect of pH, salts and sugars on the rheological properties of cress seed (*Lepidium sativum*) gum, Int. J. Food Sci. Technol. 48 (12) (2013) 2506–2513.

[31] C. Asawahame, K. Sutjarittangtham, S. Eitssayeam, Y. Tragoolpua, B. Sirithunyalug, J. Sirithunyalug, Antibacterial activity and inhibition of Adherence of *Streptococcus mutans* by propolis electrospun fibers, AAPS PharmSciTech 16 (2014) 182–191.
[32] T. Tsukame, M. Kutsuzawa, H. Sekine, H. Saitoh, Y. Shibasaki, Identification of polyethylene by differential scanning calorimetry: application to forensic science, J. Therm. Anal. Calorim. 57 (3) (1999) 847–851.
[33] C. Millot, L.-A. Fillot, O. Lame, P. Sotta, R. Seguela, Assessment of polyamide-6 crystallinity by DSC, J. Therm. Anal. Calorim. 122 (1) (2015) 307–314.
[34] Y. Liu, S. Chen, E. Zussman, C.S. Korach, W. Zhao, M. Rafailovich, Diameter-dependent modulus and melting behavior in electrospun semicrystalline polymer fibers, Macromolecules 44 (11) (2011) 4439–4444.
[35] N. Noshirvani, B. Ghanbarzadeh, A.A. Entezami, Effect of cellulose nanocrystal and polyvinyl alcohol on the physical properties of starch based bionanocomposite films, Iran Food Sci. Technol. Res. J. 8 (1) (2012) 49–59.
[36] P.E.F. Melo, A.P.M. Silva, F.P. Marques, P.R.V. Ribeiro, Souza Filho MdsM, E.S. Brito, J.R. Lima, H.M.C. Azeredo, Antioxidant films from mango kernel components, Food Hydrocolloids 95 (2019) 487–495.
[37] K. Rambabu G B, F. Banat, P.L. Show, H.H. Cocoletzi, Mango leaf extract incorporated chitosan antioxidant film for active food packaging, Int. J. Biol. Macromol. 126 (2019) 1234–1243.
[38] H. Wang, W. Wang, S. Jiang, S. Jiang, L. Zhai, Q. Jiang, Poly (vinyl alcohol)/oxidized starch fibres via electrospinning technique: fabrication and characterization, Iran. Polym. J. (Engl. Ed. (English Ed.) 20 (7) (2011) 551–558.
[39] Y.P. Neo, S. Ray, J. Jin, M. Gizdavic-Nikolaidis, M.K. Nieuwoudt, D. Liu, S.Y. Queket, Influence of solution and processing parameters towards the fabrication of electrospun zein fibers with sub-micron diameter, J. Food Eng. 109 (4) (2012) 645–651.
[40] E. Marsano, L. Francis, F. Giunco, Polyamide 6 nanofibrous nonwovens via electrospinning, J. Appl. Polym. Sci. 117 (3) (2010) 1754–1765.
[41] R. Nirmala, K.T. Nam, S.-J. Park, Y.-S. Shin, R. Navamathavan, H.Y. Kim, Formation of high aspect ratio polyamide-6 nanofibers via electrically induced double layer during electrospinning, Appl. Surf. Sci. 256 (21) (2010) 6318–6323.
[42] R. Nirmala, H.R. Pant, C. Yi, K.T. Nam, S.-J. Park, H.Y. Kim, R. Navamathavan, Effect of solvents on high aspect ratio polyamide-6 nanofibers *via* electrospinning, Macromol. Res. 18 (8) (2010) 759–765.
[43] R.N. Oliveira, M.C. Mancini, F. Oliveira, T. Passos, B. Quilty, R. Thiré, G. McGuinness, FTIR analysis and quantification of phenols and flavonoids of five commercially available plants extracts used in wound healing, Matéria (Rio de Janeiro) 21 (2016) 767–779.
[44] D.P. Suhas, H.M. Jeong, T.M. Aminabhavi, A.V. Raghu, Preparation and characterization of novel polyurethanes containing 4,4′-{oxy-1,4-diphenyl bis(nitromethylidine)}diphenol schiff base diol, Polym. Eng. Sci. 54 (1) (2014) 24–32.
[45] J. Shen, Y. Li, Y. Zuo, Q. Zou, l Zhang, H. Liu, Surface modification of polyamide 6 immobilized with collagen: characterization and cytocompatibility, Int. J. Polym. Mater. 60 (2011) 907–921.
[46] A.V. Raghu, G. Anita, Y.M. Barigaddi, G.S. Gadaginamath, T.M. Aminabhavi, Synthesis and characterization of novel polyurethanes based on 2,6-bis(4-hydroxybenzylidene) cyclohexanone hard segments, J. Appl. Polym. Sci. 104 (1) (2007) 81–88.
[47] P. Supaphol, C. Mit-Uppatham, M. Nithitanakul, Ultrafine electrospun polyamide-6 fibers: effect of emitting electrode polarity on morphology and average fiber diameter, J. Polym. Sci., Part B: Polym. Phys. 43 (24) (2005) 3699–3712.
[48] J.S. Stephens, D.B. Chase, J.F. Rabolt, Effect of the electrospinning process on polymer crystallization chain conformation in nylon-6 and nylon-12, Macromolecules 37 (2004) 877.
[49] A.P. Martínez-Camacho, M.O. Cortez-Rocha, A.Z. Graciano-Verdugo, F. Rodríguez-Félix, M.M. Castillo-Ortega, A. Burgos-Hernández, J.M. Ezquerra-Brauer, M. Plascencia-Jatomea, Extruded films of blended chitosan, low density polyethylene and ethylene acrylic acid, Carbohydr. Polym. 91 (2013) 666–674.
[50] M.S. Peresin, Y. Habibi, J.O. Zoppe, J.J. Pawlak, O.J. Rojaset, Nanofiber composites of polyvinyl alcohol and cellulose nanocrystals: manufacture and characterization, Biomacromolecules 11 (3) (2010) 674–681.
[51] S. Kumazawa, T. Hamasaka, T. Nakayama, Antioxidant activity of propolis of various geographic origins, Food Chem. 84 (3) (2004) 329–339.
[52] B.M. Razavizadeh, R. Niazmand, S. Hajinezhad, E. Akbari, Physicochemical and antimicrobial properties and determination of phenols and flavonoids content of propolis from bee hives in Khorasan Razavi Province, J. Res. Innovat. Food Sci. Technol. 9 (1) (2020) 27–40 (Extended abstract in English).
[53] K. Sutjarittangtham, S. Sanpa, T. Tunkasiri, P. Chantawannakul, U. Intatha, S. Eitssayeam, Bactericidal effects of propolis/polylactic acid (PLA) nanofibres obtained via electrospinning, J. Apicult. Res. 53 (1) (2014) 109–115.
[54] E. Mascheroni, V. Guillard, F. Nalin, L. Mora, L. Piergiovanni, Diffusivity of propolis compounds in Polylactic acid polymer for the development of anti-microbial packaging films, J. Food Eng. 98 (3) (2010) 294–301.